Published in final edited form as:
Drug Des Discov. 1995 November ; 13(2): 133–154.

MODELLING THE P_{2Y} PURINOCEPTOR USING RHODOPSIN AS TEMPLATE

A. Michiel Van Rhee[a], **Bilha Fischer**[a,b], **Philip J. M. Van Galen**[a,c], and **Kenneth A. Jacobson**[a,*]

[a]NIH, NIDDK, LBC, Molecular Recognition Section, Bethesda, Maryland 20892-0810 [b]Department of Chemistry, Bar-Ilan University, Ramat-Gan 52900, Israel [c]N.V. Organon, Computational Medicinal Chemistry Group (RK2340), 5340 BH Oss, The Netherlands

Abstract

The $P2Y_1$ purinoceptor cloned from chick brain (Webb, T. *et al.* (1993) FEBS Lett., 324, 219–225) is a 362 amino acid, 41 kDa protein. To locate residues tentatively involved in ligand recognition a molecular model of the P_{2Y} purinoceptor has been constructed. The model was based on the primary sequence and structural homology with the G-protein coupled photoreceptor rhodopsin, in analogy to the method proposed by Ballesteros and Weinstein ((1995) Meth. Neurosci. 25, 366–428). Transmembrane helices were constructed from the amino acid sequence, minimized individually, and positioned in a helical bundle. The helical bundle was then minimized using the Amber forcefield in Discover (BIOSYM Technologies) to obtain the final model. Several residues that have been shown to be critical in ligand binding in other GPCRs are conserved in the $P2Y_1$ purinoceptor. According to our model the side chains of these conserved residues are facing the internal cleft in which ligand binding likely occurs. The model also suggests four basic residues (H121 in TM3, H266 and K269 in TM6 and R299 in TM7) near the extracellular surface that might be involved in ligand binding. These basic residues might be essential in coordinating the triphosphate chain of the endogenous ligand adenosine 5′-triphosphate (ATP). Potential binding sites for agonists have been explored by docking several derivatives (including newly synthesized N^6-derivatives) into the model. The N^6-phenylethyl substituent is tolerated pharmacologically, and in our model this substituent occupies a region predominantly defined by aromatic residues such as F51 (TM1), Y100 (TM2) and F120 (TM3). The dimethylated analogue of ATP, N^6,N^6-dimethyl-adenosine 5′-triphosphate, is less well tolerated pharmacologically, and our model predicts that the attenuated activity is due to interference with hydrogen bonding capacity to Q296 (TM7).

Keywords

Molecular modelling; sequence analysis; ATP receptor(s); purinoceptor; nucleotides; G-protein coupled receptors

*Correspondence to: Dr. K. A. Jacobson, Bldg. 8A, Rm. B1A-19, NIH, NIDDK, LBC, Bethesda, MD 20892-0810.

The coordinate files for the molecular models described in this article will be included in the CD-ROM edition of the journal. The files are also available from the Editor.

INTRODUCTION

About twenty years ago Burnstock proposed the 'purinergic hypothesis' which suggested that extracellular ATP is responsible for a variety of pharmacological effects mediated via membrane bound receptors. These purinoceptors were divided into P_1 and P_2 subclasses that differentiate receptors for adenosine and ATP, respectively.[1] Pharmacological effects of extracellular ATP are exerted in peripheral tissues,[4] where ATP acts as a neurotransmitter at autonomic neuromuscular junctions,[2] as well as within the central nervous system.[3]

The family of P_2 receptors consists of no fewer than five (and likely many more) subtypes. P_{2X} (excitatory ion channel), P_{2Y} (inhibitory G-protein coupled), P_{2U} (G-protein coupled and responding to UTP), P_{2Z} (opens membrane pore in mast cells), and P_{2T} subtypes (ADP receptor on platelets) have been defined and characterized.[4–8] This classification was made on the basis of functional responses and agonist specificity. Recently, a reorganization of the nomenclature has been proposed,[8] in which all of the G-protein coupled purinoceptors are to be considered subtypes within a 'P2Y superfamily", and all of the ion channel purinoceptors are to be considered subtypes within a "P2X superfamily". The most well-established second messenger system for the metabotropic P_{2Y} and P_{2U} receptors is activation of phospholipase C via coupling to G-proteins.[9–11] ATP acting at P_{2X} receptors activates Ca^{2+} channels in smooth muscle.[12,13]

The complete elucidation of P_2 subtypes and mechanisms of action have been impeded by the limited number of stable and selective agonists and antagonists available. We have recently reported the synthesis of a variety of ATP analogues modified at either the ribose or the purine, including a series of functionalized congeners based on the potent P_{2Y} purinoceptor agonist 2-methylthioadenosine 5′-triphosphate (2MeSATP).[14,15] The 2-thio-ether derivatives were shown to be potent P_{2Y} purinergic ligands stimulating the production of inositol phosphates in turkey erythrocyte membranes with $K_{0.5}$-values ranging from 1.5 to 770 nM. Moreover, N^6-methyl-2-(5-hexenylthio)-ATP was shown to be a potent and selective P_{2Y} agonist ($K_{0.5} = 26 \pm 7$ nM). Since substitution at the N^6 position of the adenine moiety seemed to convey selectivity for a specific P_{2Y} receptor subtype,[14,15] we now synthesized the 5′-mono- and triphosphates of N^6,N^6-dimethyl-adenosine and N^6-(2-phenylethyl)-adenosine. Progress in the development of antagonists has also been made recently.[16–18]

A very characteristic feature of G-protein coupled receptors (GPCRs) is their overall topology. They all have similar hydrophobicity profiles[19] with seven stretches of increased hydrophobicity, most probably corresponding to α-helical regions spanning the cell membrane.[20] The new potent and, in some cases, selective P_2 agonists, together with the recent elucidation of the ammo acid sequences of the chick and turkey P_{2Y} purinoceptor[21,22] and the related mouse, rat and human P_{2U} purinoceptor,[23–25] encouraged us to proceed in our research effort towards understanding of the 3D structure of P_2 purinoceptors, as well as towards identification of the ligand binding site. Unfortunately, isolation, purification and crystallization of P_2 purinoceptors, as for other GPCRs, remains to be demonstrated. Not only is a crystallographic structure as yet unobtainable, but the very limited quantities of receptor protein present in the membrane, and isolation problems, prohibit the use of modern techniques, such as nuclear magnetic resonance spectroscopy, towards structure elucidation. Chemical modification of the ligand binding site and site-directed mutagenesis have been shown to be useful techniques in understanding receptor-ligand interactions,[26] but is in the case of P_2 purinoceptors restricted by the lack of suitable radioligands. A possible further approach is to construct models of the receptors and their ligand complexes using molecular modelling, as was first proposed by Hibert *et al.*[27] In this paper we present a model of the chick P_{2Y} purinoceptor based on the electron density map of rhodopsin,[28] rather than on the

bacteriorhodopsin template[29] used by Hibert *et al.*[27] The model is verified by incorporation of site-directed mutagenesis [41,50,51] and ligand affinity data.[14,15]

MATERIALS AND METHODS

Computational Methods

Software and hardware—Calculations and manipulations were performed using the Quanta (Molecular Simulations Inc., Sunnyvale, CA, releases 3.1.1 and 4.0) and Insight II (BIOSYM Technologies, San Diego, CA, version 2.2.0) modelling packages. All minimization calculations, on either proteins or the ligand-receptor complex, were performed using the Amber forcefield in Discover (BIOSYM Technologies, San Diego, CA, version 2.90). Single ligands were minimized using the MNDO hamiltonian in the MOPAC program (Quantum Chemistry Program Exchange, version 6.0). The Sequence Analysis Software Package of the Genetics Computer Group (University of Wisconsin, Madison, WI, version 7.3.1-UNIX) was used for producing the Kyte-Doolittle, surface probability, helical wheel and dendrogram analyses. The MOPAC program was run on a Convex C3830 system (Convex Computer Corp., Richardson, TX) and GCG was run on an SGI Challenge XL (Silicon Graphics Inc., Mountain View, CA, MIPS R4400 CPU). All other programs were run on an Iris Indigo XZ4000 (Silicon Graphics Inc., Mountain View, CA, MIPS R4000 CPU) workstation.

Model building—The sequences for the chick and turkey P_{2Y} purinoceptor were taken from Webb *et al.*[21] and Filtz *et al.*,[22] respectively, and the sequences for the mouse, rat, and human P_{2U} receptor were taken from Lutstig *et al.*,[23] Rice *et al.*,[25] and Parr *et al.*,[24] respectively. Kyte-Doolittle hydrophobicity and Emini surface probability parameters were calculated using a 7 amino acid window. With these parameters, the putative transmembrane domains were identified. A sequence homology search was performed on the third transmembrane domain of the chick P_{2Y} sequence (see discussion), using the World Wide Web version of the Basic Logical Alignment Search Tool (National Center for Biotechnology Information (NCBI), Bethesda, MD). Sequences were obtained from the Swiss, GenPept, EMBL, or PIR databases maintained by the NCBI. Sequences of the putative transmembrane domains (TMs) were aligned manually using the P_{2Y}, P_{2U}, and rhodopsin sequences based on common patterns, rather than on amino acid homology alone. The alignment for bacteriorhodopsin was based on the procedure developed by Oliveira *et al*[30] The identifier for the first TM was either GX_3N or GN where X represents any occurring amino acid. The identifiers for TM2 through TM7 were LX_3DX_7P or LX_3DX_8P (TM2), $SX_3LX_2IX_2DR$ (TM3) or $SX_3LX_2IX_2Hr$, WX_8P or WX_9P (TM4), FX_2PX_7Y (TM5), FX_2CX_2P (TM6) and $LX_3NX_3DPX_2Y$ or $LX_3NX_3NPX_2Y$ (TM7), respectively.

Helices were built from the full length of the TM, using the Biopolymer module in the Insight II program. The N terminus was capped with an acetamido group, and the C terminus was capped with a carboxamido group. The secondary structure was assumed to be a right-handed alpha helix (default ϕ and Ψ angles from the Biopolymer module). After generation of the Amber atom type parameters and template charges, the helices were energy minimized as described in the Energy Minimization section.

The energy minimized helices were converted to Protein Database Brookhaven (PDB) format files and imported in the Quanta program. Coils (an alpha carbon backbone representation of the helix) of the minimized helices were drawn, that resemble the helical wheel representation to aid in orienting the individual helices towards each other.

The following constraints were used constructing the helical bundle:

1. The helical axes of the first, third, fifth and seventh helices were quasi-antiparallel to those of the second, fourth and sixth helices.
2. The hydrophobic side of each helix was facing the lipid phase and the hydrophilic side of each helix was facing either another helix or the pore formed by the helical bundle.
3. Conserved residues, either identical throughout a subset or highly homologous, determined the orientation of each helix relative to the other helices.
4. Distances in the electron density map of rhodopsin[28] correlated to atomic coordinates in the model. This was obtained through triangulation of the electron density map and conversion of the coordinates to a grid on the screen.
5. The assembly of helices maintained a clockwise order, when seen from the intracellular side, as argued by Baldwin.[31]
6. None of the helices were intersecting.

The helical bundle was then energy minimized as described in the Energy minimization section.

Energy minimization—The individual helices generated with Insight II's Biopolymer module were energy minimized in Discover using a stepwise process. Initially, 200 steps of Steepest Descent were performed, followed by minimization using the Conjugate Gradient (CG) method until the gradient reached a value below 0.1 kcal/mol/Å. Use of the Amber forcefield in Discover required that in all calculations the 1–4 nonbonded interactions were scaled by a factor 0.5, and the dielectric constant was assumed to be distance independent with a magnitude of 4. The bond, theta, phi, out-of-plane, nonbonded and Coulombic interactions were all used to obtain the final energy, but were not expressly scaled.

The helical bundles generated with Quanta were energy minimized in Discover in a stepwise process. Initially, 500 steps CG were performed with the backbone of the helices tethered with a force constant of 100 kcal/Å. In consecutive runs (500 steps CG each), the force constant was reduced to 50 kcal/Å, then 25 kcal/Å and, finally to 0 (no tethering).

Ligand docking—Six ligands were used to probe the receptor for possible ligand binding domains (BDs). Adenosine 5′-triphosphate (ATP) was constructed from guanosine 5′-(3-thiotriphosphate) co-crystallized with transducine[38] and modified using the Builder module of Insight II (see discussion). 2-Methylthio-adenosine 5′-triphosphate (2MeSATP), 2-(2-(4-aminophenyl)ethyl)thio-adenosine 5′-triphosphate (APSATP), N^6-(2-phenylethyl)-adenosine 5′-triphosphate (N^6PEATP), N^6,N^6-dimethyl-adenosine 5′-triphosphate (N^6diMeATP), and triphosphate were constructed from ATP using the Builder module of Insight II. The ligands were then fully minimized using the MNDO hamiltonian of MOPAC. All ligands were rigidly docked into the helical bundle using graphical manipulation coupled to continuous energy monitoring, *i.e.* the ligand was manually docked into the binding site without relaxing the atomic coordinates of either ligand or protein while, continuously, calculating the energy of the whole. When a final position was reached, consistent with a low local energy and known pharmacological data, the complex of receptor and ligand was subjected to a minimization run of 4000 steps CG (or until the gradient was < 0.1 kcal/mol/Å). Charges for the ligands were imported from the MOPAC output files.

Empirical Methods

Synthesis—New compounds were characterized by proton nuclear magnetic resonance using a Varian GEMINI-300, a Bruker AM-300 or a Bruker AC-200 NMR spectrometer.

Spectra were taken in D_2O. In all cases H-2′ was associated with the water peak. Nucleotides were also characterized by ^{31}P NMR in D_2O using H_3PO_4 as an external reference. Samples were treated with CHELEX-100 (BioRad, Richmond, CA) prior to measurement. Nucleotides were desorbed from a glycerol matrix under fast atom bombardment (FAB) conditions using 6 kV Xe atoms on a Joel SX102 spectrometer. Preparation of tri-n-butylammonium pyrophosphate for the triphosphate synthesis, as well as the preparation of triethylammonium bicarbonate (TEAB) buffer was done as published.[14,15] Purification of nucleotides was achieved on an Isco UA-6 LC system using DEAE A-25 Sephadex columns and a linear gradient of 0–0.4 or 0.6 M NH_4HCO_3. Peaks were detected by UV absorption at 280 nm. The final purification was done on a Hewlett-Packard 1090 HPLC system using a semipreparative SynChropak RPP-100 column (10 × 250 mm, SynChrom, Inc., Lafayette, IN) with a flow rate of 3 ml/min. For analytical purposes, a nucleoside/nucleotide 7U column (4.6 × 250 mm, Alltech Associates, Inc., Deerfield, IL) was used with a flow rate of 1 ml/min. Separation was obtained using either a linear gradient of 0.1 M triethylammonium acetate buffer (TEAA, pH = 8.3) and acetonitrile (20% to 60% in 20 min; solvent system I) or 60 mM ammonium phosphate and 5 mM tetrabutylammonium phosphate (TBAP) in 90% water/10% methanol and 5 mM TBAP in methanol (25% to 75% in 8 min; solvent system II). Peaks were detected by UV absorption at 260 nm, and spectra collected with a diode array detector. Nucleotides were generally > 90 % pure. N^6,N^6-dimethyladenosine was purchased from Sigma (St. Louis, MO), and N^6-(2-phenylethyl)adenosine was from Research Biochemical International (Natick, MA).

N^6-(2-phenylethyl)-adenosine 5′-monophosphate bis-triethylammonium) salt (**1**, N^6PEAMP) and *N^6-(2-phenylethyl)-adenosine 5′-triphosphate tetrakis-(triethylammonium) salt* (**2**, N^6PEATP): The procedure for nucleoside triphosphate synthesis was adapted from Kovács and Ötvös[32] and Moffat.[33] The reaction was carried out on 25 mg (0.067 mmol) of N^6-2-phenylethyl-adenosine. The reaction mixture was then lyophilized and separated on a Sephadex DEAE A-25 column using a 0–0.5 M NH_4HCO_3 linear gradient. The monophosphate product **1** was obtained in 76% yield (25 mg). HPLC chromatography (nucleoside/nucleotide 7U column; solvent system II) showed > 98% purity. Retention time: 6.36 min. ^1H NMR (D_2O) δ 8.50 (1H, s, H-8), 8.13 (1H, s, H-2), 7.26 (5H, m, Ph), 6.06 (1H, d, J = 6 Hz, H-1′), 4.46 (1H, t, J = 6 Hz, H-3′), 4.31 (1H, m, H-4′), 3.95 (2H, t, J = 4 Hz, H-5′), 3.85 (2H, m, CH_2NH), 2.98 (2H, t, J = 7.2, Hz, CH_2Ph) ppm. High resolution FAB: calculated for $C_{18}H_{19}N_5O_7P_1$ 450.1173, found 450.1179.

The triphosphate product **2** was obtained in 21% yield (10 mg). This product was further purified on a semipreparative SynChropak RPP-100 column (solvent system I), and obtained in > 90% purity. Retention time (nucleoside/nucleotide 7U column; solvent system I) 4.13 min. ^1H NMR (D_2O) δ 8.50 (1H, s, H-8), 8.15 (1H, s, H-2), 7.28 (5H, m, Ph), 6.08 (1H, br.s, H-1′), 4.52 (1H, t, J = 6 Hz, H-3′), 4.38 (1H, m, H-4′), 3.22 (2H, m, H-5′), 3.87 (2H, m, CH_2NH), 2.95 (2H, t, J = 7 Hz, CH_2Ph) ppm. High resolution FAB: calculated for $C_{18}H_{23}N_5O_{13}P_3$, 610.0525, found 610.0505.

N^6,N^6-dimethyl-adenosine 5′-monophosphate bis-(triethylammonium) salt (**3**, N^6diMeATP) and *N^6N^6-dimethyl-adenosine 5′-triphosphate tetrakis-(triethylammonium) salt* (**4**, N^6diMeATP): The reaction was carried out on 25 mg (0.054 mmol) of N^6,N^6-dimethyl-adenosine. The reaction mixture was lyophilized and separated on a Sephadex DEAE A-25 column using a 0–0.5M NH_4HCO_3 linear gradient. The monophosphate product 3 was obtained in 62% yield (19.3 mg). This product was obtained upon purification on a semipreparative SynChropak RPP-100 column (solvent system I) resulting in > 98% purity. Retention time (nucleoside/nucleotide 7U column; solvent system I) 2.55 min. ^1H NMR (D_2O) δ 8.51 (1H, s, H-8), 8.18 (1H, s, H-2), 6.10 (1H, d, J = 5.6 Hz, H-1′), 4.45 (1H, m,

H-3′), 4.32 (1H, m, H-4′), 3.95 (2H, t, J = 4 Hz, H-5′), 3.42 (s, 6H, Me) ppm. High resolution FAB: calculated for $C_{12}H_{17}N_5O_7P_1$ 374.0888, found 374.0866.

The triphosphate product **4** was obtained in 5% yield (2.5 mg). This product was obtained upon purification on a semipreparative SynChropak RPP-100 column (solvent system I) resulting in > 98% purity. Retention time (nucleoside/nucleotide 7U column; solvent system I) 2.8 min. ^{1}H NMR (D_2O) δ 8.46 (1H, s, H-8), 8.20 (1H, s, H-2), 6.12 (1H, d, J = 5.7Hz, H-1′), 4.60 (1H, m, H-3′), 4.39 (1H, m, H-4′), 4.20 (2H, t, J = 4 Hz, H-5′), 3.44 (s, 6H, Me) ppm. High resolution FAB: calculated for $C_{12}H_{19}N_5O_{13}P_3$ 534.0167, found 534.0192.

Pharmacology—The biological characteristics of the novel compounds, determined using standard methodology,[10,14] will be published separately.[56]

RESULTS AND DISCUSSION

The $P2Y_1$, purinoceptor cloned from chick brain[21] is a 362 amino acid, 41 kDA protein that shares < 20% identity with adenosine receptors. We built a model of this receptor in order to locate residues tentatively involved in ligand recognition and signalling. The steps of approach consisted of 1) Defining approximate boundaries of the helical regions from Kyte-Doolittle plots[19] and from determination of sequence homology to other receptors (Figures 1 and 2). This also established which residues of P_2 receptors correspond to those that have been postulated to be involved in ligand recognition in other receptors,[41,46,47,48,50,51] and are, therefore, directed toward the binding site. This was useful for proper rotation of the helices.; 2) Building the receptor model using rhodopsin,[31] with which it shares sequential and structural homology, as a template.[34] Transmembrane helices were constructed from the amino acid sequence, minimized individually, and positioned in a helical bundle; and 3) Docking of ATP and synthetic analogues.[14,15] For this purpose we have prepared, in addition to the already published compounds, the mono- and triphosphate analogues of N^6-(2-phenylethyl)- and N^6,N^6-dimethyl adenosine, as probes of the N^6 region in the P_{2Y} receptor binding site.

Alignment with other G protein-coupled receptors and dendrogram

A dendrogram (Figure 1) composed for the sequences of 29 G protein-coupled receptors (including orphan receptors) and bacteriorhodopsin shows that the known metabotropic P_2 receptor sequences (P_{2Y} and P_{2U}) are more closely related to each other than to any other receptor. Comparison of the P_{2Y} (chick) and P_{2U} (rat) receptor subtypes with other GPCR sequences showed only low percentages of sequence identity (e.g., angiotensin II – P_{2Y} 27%, angiotensin II – P_{2U} 22%, thrombin – P_{2Y} 25%, thrombin – P_{2U} 25%; interleukin 8 – P_{2Y} 22%; interleukin 8 – P_{2u}; 23%). Both P_{2Y} and P_{2U} receptors bear a marginal sequence identity with the A_1 adenosine (21% for P_{2Y} and less than 12% for P_{2U}) or cAMP receptors (17% for P_{2Y} and less than 12% for P_{2U}). A comparison of P_{2Y} vs. P_{2U} receptors revealed 38.8% identity and 58.6% similarity. In the transmembrane regions the identity percentage was even higher - 52%. Also, the P_2 receptors are only distantly related to the biogenic amine receptors. An alignment of selected sequences (Figure 2) was constructed. The patterns on which this alignment is based differ markedly between the biogenic amine subclass and the P_{2Y} and P_{2u} type receptors.

In TM1, the motif GXXXN (P_{2Y}) or GXXGN (P_{2U}) occurs rather than the GN motif in the biogenic amine receptors. The alternate motifs, however, are not exclusively used by P_2 receptors, but are shared with, e.g., the PGE_3-II (GXXGN) and the PAF (GXXXN) receptors. In all sequences the last 5 C-terminal residues of this helix are frequently occupied by lysine or arginine residues, indicating the end of the transmembrane domain.

Such basic residues may serve as 'membrane anchors',[34,32] and are useful in determining the position of the helix in the lipid bilayer.

In TM2, the residue preceding the conserved leucine in the LXXXD motif is a conserved serine for the biogenic amine receptors, but is either an asparagine or a histidine in the P_{2Y} and P_{2U} receptors, respectively. The asparagine is conserved among the P_{2Y}, AT_{1A}, CKR1, IL-8A, PAF, NK2 receptors, the opsins and rhodopsin. The histidine is shared between P_{2U} and thrombin receptors. Another difference between biogenic amine receptors and P_2 receptors is the position of the conserved proline relative to the conserved aspartate. Although absent in the muscarinic receptor, the proline is consistently spaced by 8 residues from the aspartate in the other biogenic amine receptors, whereas in many other receptors, the P_2 receptors included, only 7 residues separate these two residues. This last difference is possibly significant since the proline is located near the luminal side of the receptor protein, which is thought to be important for ligand binding. The only exceptions, observed so far, to the conservation of the aspartate occur in the substance P receptor where it is substituted with a glutamate, and in the gonadotropin-releasing hormone receptor where an asparagine replaces this residue. It has been argued by Zhou *et al.*[52], that the conserved aspartate in TM2 is in close proximity to the conserved asparagine in TM7, and that the concurrent change of D to N in TM2 and N to D in TM7 in the gonadotropin-releasing hormone receptor is consistent with this finding. However, all P_{2Y} and P_{2U} receptor sequences identified so far, and several other receptors such as the TXA_2, thrombin, PAF, and PGE_3-II receptors, contain an aspartate in both TM2 and TM7. This argues against the hypothesis of close proximity of the two residues, which is indeed found in our model of the chick $P2Y_1$ receptor. The conserved aspartate in TM2 was shown by Horstman *et al.* [53] to be a sodium-dependent allosteric regulatory site in the α_2-adrenergic receptor.

The DRY motif, characteristic of the third transmembrane domain in biogenic amine receptors, is replaced by a HRY motif in the P_2 GPCRs. This motif has not been found in other receptors. The only substitution for the conserved aspartate, seems to be the D to E in *e.g.*, the TXA_2, PGE_3-II, opsin and rhodopsin sequences. The significance of this deviation is not clear, but is supposedly important for coupling of the P_2 receptors to G-proteins and not for ligand binding, the subject of this study.

One or more of the first 6 positions in the N-terminal sequence of TM4 are generally (37 out of 40 aligned sequences of family A GPCRs) occupied by lysine or arginine residues. Again these residues could well serve as 'membrane anchors'. They seem to be occurring more frequently towards the cytosolic side of helices than on the luminal side, thus reflecting the polarity of the membrane. These 'membrane anchors' also occur much less frequently in the C-terminal sequences of helices, than in the N-terminal sequences as is demonstrated by the alignment for TM5. The reason for this disparity is believed to be the direction in which the side-chains are pointing, *i.e.* opposite to the propagation direction of the helix, allowing more rotational freedom for lysine and arginine residues near the cytosolic N-terminus than for the cytosolic C-terminus. There are no other marked differences between the various receptor subfamilies for either TM4 or TM5.

The CXXP motif used for the alignment of TM6 could be substituted by WXP for most receptors, but the P_2 receptors deviate at this position. The P_{2Y} receptor has a tyrosine at the position of the conserved tryptophan, and this seems to be rather unique. The phenylalanine in the P_{2U} receptor at the same position occurs more frequently, such as in the thrombin, and various orphan receptors. Characteristic of the P_2 receptors is the presence of a lysine (P_{2Y}: K269) or an arginine (P_{2U}: R265) at an otherwise non-conserved position. It shares this feature only with the endothelin receptors (both ET-A and ET-B subtypes) and the orphan

receptor RSC338. The proposed 'membrane anchors' occur quite frequently at the first position in the alignment of this transmembrane domain.

TM7 is best aligned by means of the NPXXY motif. However, the P_2 receptors, the gonadotropin-releasing hormone receptor, the TXA_2, PGE_3-II, and several orphan receptors constitute an exception to this rule. The conserved asparagine is replaced by an aspartate residue in the latter cases. A non-conserved aspartate (D352) in the $5HT_{1B}$ receptor aligns perfectly with aspartates in the IL-8A receptor (D288), and in the D_{1B} receptor (D342), a glutamine in the P_{2Y} receptor (Q296) and a lysine in the P_{2U} receptor (K289). Arginines 299 (P_{2Y}) and 292 (P_{2U}) align with Y530 in the m3, E291 in the IL-8A and E287 in the CKR1 receptor, respectively. Both positions are near the luminal side of the receptor and are likely involved in ligand binding. The K and R residues occurring near the C-terminus are probably better characterized as 'membrane anchors'.

According to Abbracchio *et al.*,[8] the chick P_{2Y} and turkey P_{2Y} receptors should be classified as $P2Y_1$ and $P2Y_4$, respectively, based on their pharmacological profile. On the basis of the currently available sequences however, this subclassification is redundant since the two sequences differ only at position 28 in the N-terminus of the sequences. The chick threonine residue is replaced by the highly homologous serine residue in the turkey sequence. Any pharmacological difference would be methodological rather than sequence related. The mouse, rat, and human P_{2U} ($P2Y_2$) receptors are much more divergent, as is illustrated by the dendrogram (Figure 1). The P_2 receptors, regardless of subtype, whether GPCR or ligand-gated ion channel, are often regarded as related to the better characterized and more widely known adenosine receptors [Burnstock[4] and most subsequent reviews]. From the dendrogram (Figure 1), however, it must be concluded that, *e.g.*, the A_{2a} adenosine receptor is more closely related to the biogenic amine receptors, than to any of the GPCR P_2 receptors. The P_2 receptors are more closely related to the PAF, AT_{1A}, and IL-8A receptors, and various orphan receptors, than to any other GPCR subfamily. Bacteriorhodopsin, included to facilitate comparison with other modelling studies, [e.g., 27,35] is clearly not related to any of the GPCR subfamilies. The degree of relatedness between bacteriorhodopsin and GPCRs shown in the dendrogram is probably an overestimate of the actual distance, caused by the residue alignment procedure of the program.

Kyte-Doolittle hydrophobicity and Emini surface probability analysis

At the portion of the sequence where proteins are supposed to cross the lipid bilaycr membrane, the hydrophobicity of that segment is usually increased relative to the cytosolic and luminal portions. The procedure developed by Kyte and Doolittle[19] uses this phenomenon to identify transmembrane domains in protein sequences with unknown structure. In the case of GPCRs, these transmembrane domains are thought to be alpha helical, and more importantly amphiphilic. The amphiphilicity of the TMs supposedly reflects the way a GPCR is built out of seven of these helical transmembrane domains. Consequentially, the hydrophobicity profile of these GPCRs is not as clear as one would wish. An example of this effect is the poor separation of the sixth and seventh TM in both the P_{2Y} receptor profile and the bacteriorhodopsin profile (data not shown). To facilitate identification of TMs, the Kyte-Doolittle hydrophobicity method is often supplemented with methods describing other sequence dependent vectorial parameters, such as the 'conservation moment' and 'hydrophilic moment',[36] for each helix or other computational methods[43]. Use of the 'conservation moment' method requires a particularly well defined alignment of highly homologous sequences, and can not be applied to the P_2 GPCRs because of the low sequence similarity of these receptors with any other GPCR subfamily. The 'hydrophilic moment' method relies on a database of partial hydrophilic factors for any given amino acid and is dependent on the method with which these factors were measured. Furthermore, the high incidence of basic residues in the P_{2Y} receptor sequence greatly

influences the results obtained with this method. In contrast, the Emini surface probability can be calculated from a given sequence, indicating the propensity of a stretch of amino acids (the window) to be at the surface of a protein. The combination of an increase in the Kyte-Doolittle hydrophobicity index and a decrease in the Emini surface probability index was successfully applied to predict the TMs in the P_{2Y} receptor and in the reference protein bacteriorhodopsin. The start and end residue of each helix was usually predicted within 3 residues of the TMs used by Henderson *et al.*[29] The only deviation from ideality that could not easily be explained by invoking the actual sequence, is the propagation of TM2 in bacteriorhodopsin 9 residues beyond its established terminating residue. Three other deviations could be explained by a closer examination of the profiles with regard to the sequence. The only major deviation in the P_{2Y} receptor prediction occurred at the N-terminus of TM7. This particular sequence contains 3 hydrophilic residues (K, Q and R) that are possibly involved in ligand binding, thus delaying the start of the predicted TM.

Building the receptor model

Modelling of G protein-coupled receptors has become an important tool in understanding drug-receptor interactions and in the development of new ligands for these receptors. The first widely accepted method was the homology modeling method by Hibert *et al.*[27] This method involved the alignment of the receptor sequence with the sequence of bacteriorhodopsin, and the subsequent mapping of the sequence onto the structure of bacteriorhodopsin that was determined by Henderson *et al.*[29] Bacteriorhodopsin is a proton pump in the outer membrane of *Halobacterium halobium*, and lacks any functional or sequence homology with GPCRs. Nevertheless, the procedure was based on the assumption that there would be considerable structural homology. This structural homology was inferred by the extraordinary similarity in the hydrophobicity plots, or Kyte-Doolittle plots, of the biogenic amine subfamily of GPCRs and bacteriorhodopsin. Recently, a low resolution electron density map of rhodopsin, a true member of the GPCR superfamily, was published.[28] The low sequence homology with bacteriorhodopsin, the structural differences that must arise from the different placement of proline residues (causing bends in helices) in bacteriorhodopsin- and GPCR-sequences, and the availability of an electron density map of a true member of the GPCR superfamily prompted us to adapt a new method to build models of GPCRs.[34] This novel method is based on a computational approach rather than strict compliance with the atomic coordinates of a distantly related protein, albeit with higher resolution.

To ascertain the viability of modelling transmembrane proteins (based on the structure of rhodopsin[34]) by the methods described in this paper, we built models of bacteriorhodopsin (data not shown) based on the electron density map of bacteriorhodopsin,[29] and rhodopsin (data not shown) and the P_{2Y} receptor based on the electron density map of bovine rhodopsin as published by Schertler *et al.*[28] root mean square (r.m.s.) distance calculations on superimposed structures were performed to establish how well the models fitted the experimental data. The bacteriorhodopsin model that was constructed, compared with the one deposited in the PDB,[29] had an r.m.s. value of 2.15 Å when measured on all backbone atoms and 2.06 Å on all C^{α} atoms.

Both values are lower than the resolution of the model, i.e. 3.5 Å. When the rhodopsin model was compared with the bacteriorhodopsin model by Henderson *et al.*,[29] however the r.m.s. value increased to 16.96 Å when measured on all backbone atoms and 16.86 Å on all C^{α} atoms. These rather high values indicate that there are more structural differences between bacteriorhodopsin and rhodopsin than have been assumed thus far [44] In our opinion, the position of the proline residues in the helices is a major determinant in this mater. As can be seen from the alignment for the helices, proline residues occur less frequently and at different positions in the sequence of bacteriorhodopsin than in the

sequence of rhodopsin. The influence of proline residues in α-helices was extensively studied by Sankararamakrishnan and Vishveshwara[37] and von Heijne.[45] We have found that applying the Amber forcefield to our calculations yields results in agreement with Sankararamakrishnan and Vishveshwara[37] and von Heijne,[45] and that those results are consistent with data obtained from a crystallographic study of the transmembrane protein photosynthetic reaction center (PDB: 1prc) and globular proteins such as phosphoglycerate kinase (PDB: 3pgk), lysozyme (PDB: 1127) and alcohol dehydrogenase (PDB: 5adh). The differences between the structures derived from the electron density maps of bacteriorhodopsin and rhodopsin also illustrate why helical wheel models, widely used by molecular biologists, are highly imprecise when applied to GPCRs.[31]

Ligand docking

Figure 3 represents the final helical bundle with ATP docked into the purported ligand binding cavity. It is viewed from the luminal or extracellular side, as opposed to the rhodopsin template that was determined from the intradiscal or intracellular side. The backbones of the helices are accentuated with ribbons to emphasize the tilt of the helices towards each other and the effect of prolines in the sequence. Marked kinks are visible in, *e.g.*, TM2 and TM4. ATP, which is significantly larger than the biogenic amine neurotransmitters, occupies the binding cleft formed by helices 2, 3, 5, 6, and 7. TM4, in particular, seems to be located too far outward to participate in ligand binding. Figure 4 is an cut-away drawing of TMs 5–7, shown to contain multiple ligand binding residues in the A_{2a} receptor.[51] The binding of the endogenous ligand ATP seems to occur around the upper third to upper half of the helical bundle. ATP is oriented in the plane of the lipid bilayer, almost perpendicular to the TMs. Figure 4 also demonstrates the use of 'membrane anchors' near the bottom of TM5 and TM7, and the top of TM6. Figure 5 focuses on the ligand binding domain (BD) formed by TMs 5–7. Although not directly involved in ligand binding, Pro218 in TM5 and Pro264 in TM6 have a great impact on receptor structure, and therefore, the BD. They are both located at the same distance from the membrane surface as the ligand and, more importantly, Phe215 and Phe219, located at opposite sides of the discontinuity formed by Pro218, are in close proximity of the terminal phosphate of ATP. This particular geometry is highly suggestive of the much heralded, but as yet unproven conformational change induced by agonists.

Ligand docking was initially performed with ATP, using a typical conformation based on crystallographic data for protein-bound nucleotides. To avoid the characteristically curled conformation of the triphosphate chain found in several phosphate, transferases, we opted to use the nucleotide bound to the phosphate hydrolase transducin,[38] even though it involved substituting the purine guanine with the purine adenine. The orientation of the adenine moiety relative to the ribose ring was anti (*i.e.*, the dihedral angle χ C9-N9-C1′-O4′ was 30.18°). The ring puckering, defined by the dihedral angle C1′-C2′-C3′-C4′ was, −3.85°, resulting in a 2′-exo, 3′-endo conformation for the two hydroxyl groups. After energy minimization the receptor was probed for possible hydrogen bonds (up to 5 Å between heavy atoms), electrostatic interactions (up to 10 Å between heavy atoms), and aromatic interactions (up to 10 Å between heavy atoms) There appeared to be only one favourable interaction between the adenine moiety of ATP and the receptor. The side chain of Gln296 (TM7) was within hydrogen bonding distance of the N^6 atom at 4.51 Å. More residues were tentatively involved in coordinating the ribose moiety. The side chain of Ser306 (TM7) and the O2′ are separated by only 3.03 Å. The side chain of Ser306 (TM7) is within hydrogen bonding distance of 02′ at 2.95 Å and O3′ at 2.84 Å and the backbone carbonyl of Ala302 (TM7) is positioned at 4.53 Å of both hydroxyl groups. Arg299 (TM7) is within range of several heavy atoms, including O5′ (2.83 Å to Nε), O1α (3.30 Å to Nε), O1β (3.69 Å to NH), 02β (3.12 Å to NH), and O3α (2.90 Å to NH). Other interactions with the triphosphate

chain seem to be constituted by His121 (TM3; 3.85 Å, Nε to O1β), Tyr125 (TM3; 2.73 Å, OH to O1β), Lys269 (TM6; 2.71 Å O3γ, 4.16 Å to O1β, and 4.49 Å, to O3β; all from Nε), and His266 (TM6; 4.91Å Nε to O1γ, 2.97 Å, Nε to O2γ and 3.77 Å, Nε to O3γ, 3.50 Å Nδ to O2γ, 3.78 Å Nδ to O3γ, and 4.64 Å Nδ to O3β). Aromatic residues can be found at 3.62 Å (O3γ to *m*-position of Phe219 in TM6),5.06 Å (03γ to *o*-position of Phe215 in TM6), 4.30 Å (C2 to *m*-position of Phe51 in TM1), 5.57 Å (C2 to *m*-position of Phe55 in TM1), and 9.98 Å (C2 to *m*-position of Tyr47 in TM1). Of special interest are four basic residues (His121 in TM3, His266 and Lys269 in TM6, and Arg299 in TM7) near the extracellular side of the helical bundle. In our model these residues are essential to coordinate the triphosphate moiety of the natural ligand ATP. Experimental support for this hypothesis was not only granted by experiments by Erb *et al.*,[41] but also derived from the alignment and sequence analysis of over 40 GPCRs. Erb *et al.*[41] showed that residues His262 (TM6), Arg265 (TM6) and Arg292 (TM7) in the human P_{2U}, receptor (corresponding to His266 (TM6), Lys269 (TM6) and Arg 299 (TM7) in the P_{2Y} purinoceptor, respectively) are directly involved in receptor activity. This was also the case for Lys289 (TM7; Gln296 in the P_{2Y} receptor), but the difference in character between a lysine (P_{2U}: UTP) and a glutamine (P_{2Y}: ATP) residue suggests different functions in the mode of binding of the respective ligands. Tyr114 (TM3; Hisl21 in the P_{2Y} receptor) was not investigated in the study, but the importance of this residue emerged from the modelling work. The central position of TM3 in the rhodopsin template, the distance from the extracellular surface, and the hydrogen bonding capacity of both histidine and tyrosine are all consistent with a role in ligand binding. H262 in the P_{2U} receptor,[41] H250 in the A_{2a} receptor,[51] and H265 in the NK1 receptor,[50] the equivalents of H266 (TM6) in the P_{2Y} receptor, were all shown to be important for ligand binding. The same holds true for R265 (P_{2U}), N253 (A_{2a}) and F268 (NK1) [the equivalents of K269 (TM6)], K289 (P_{2U}) and Y271 (A_{2a}) [the equivalents of Q296 (TM7)], R292 (P_{2U}) and I274 (A_{2a}) [the equivalents of R299 (TM7)], H278 (A_{2a}) corresponding to S303 (TM7), and S281 (A_{2a}) corresponding to S306 (TM7). His121 (TM3; P_{2Y}) aligns, *e.g.*, with Tyr529 in the rat m3,[46] Asn412 in the human β_2,[47] and Thr355 in the human $5HT_{1B}$ receptor,[48] and all residues were shown to be essential for agonist binding. In contrast, Lys114 (TM3) in the P_{2Y} and Lys107 (TM3) in the P_{2U} receptor were not implicated in ligand binding[41], whereas mutation of the equivalent residue, Asp99, in the rat ml receptor resulted in loss of affinity.[49] This residue is located at the fringe of the transmembrane domain or even in the first extracellular loop in our model. It is therefore likely that the residue is involved in accessibility of the ligand binding domain or in maintaining a specific structure in the loop.

In addition to ATP, we also docked N^6-(2-phenylethyl)-adenosine 5′-triphosphate (N^6PEATP), 2-(2-(4-aminophenyl)ethyl)thio-adenosine 5′-triphosphate (APSATP), N^6,N^6-dimethyl-adenosine 5′-triphosphate (N^6diMeATP), 2-methylthioadenosine 5′-triphosphate (2MeSATP) and triphosphate into the helical bundle. After minimization, the energy of all complexes was between −2500 and −2600 kcal/mol and the complexes were 400 to 500 kcal/mol more stable than the sum of the components. Since triphosphate yielded values similar to the adenosine derivatives, the energy contribution of the triphosphate moiety by far exceeds the combined contribution of the ribose and the adenine moiety. Energy differences between compounds must therefore be regarded as qualitative rather than quantitative indications of ligand affinity.

The role of divalent cations such as Mg^{2+} in P_2 purinergic transmission has been described throughout the literature.[1–11] This is not addressed in our model, because current pharmacological data are not sufficient to hypothesize the position and mechanism of such divalent cations in receptor structure. The impact of the divalent cation Zn^{2+} on binding of antagonists to the tachykinin NK-1 receptor and its mutants was recently demonstrated and described in detail by Elling *et a1.*[50]

Correlation between modelling and pharmacology

It appears that the binding of the triphosphate moiety is a major determinant in binding of ligands to the P_{2Y} purinergic receptor. Since this part of the molecule contains multiple negative charges, one would expect to find counterions in the BD. Indeed, the $P2Y_1$ receptor sequence contains several positively charged residues. Our modelling study reveals that, of these, Lys269 (TM6) and Arg299 (TM7) are likely candidates for this function and are appropriately positioned within the helical bundle to exert this function. We propose that these two basic residues are assisted by two histidine residues, His121 (TM3) and His266 (TM6), and one tyrosine residue, Tyr125 (TM3). These residues tentatively coordinate the α-phosphate (His121 and R299) the β-phosphate (Y125, K269 and R299), and the γ-phosphate (His266, and K269). Although adenosine 5′-monophosphate analogues are widely regarded as inactive at P_2 purinergic receptors,[2,5,6] Fischer *et al.*[14] recently demonstrated that one monophosphate analogue in particular, 2-(5-hexenyl)thio-adenosine 5′-monophosphate, is a more potent ($K_{0.5}$ =328 ± 43 nM; 8.5-fold over ATP) agonist at P_{2Y} receptors on turkey erythrocytes than ATP ($K_{0.5}$ = 2800 ± 700 nM). In our model there is sufficient coordination of the α-phosphate to warrant such an interaction, although the number of stabilizing interactions, and hence the interaction energy and affinity, will be lower than in the case of the corresponding triphosphate. This is pointedly illustrated by the $K_{0.5}$ values of 2-(5-hexenylthio)-ATP (10 ± 4 nM) and 2-(5-hexenylthio)-AMP (328 ± 43 nM).[14] Since the interaction between the receptor and a ligand monophosphate is much weaker than with a triphosphate, the effect of substituents at distal sites, such as in N^6PEAMP no effect ≤ 10^{-4} M) and N^6diMeAMP (no effect ≤ 10^{-4} M), increases and the combined effect of deleting two phosphates and adding N^6-substituents proved detrimental to activity. Interestingly, Erb *et al.*[41] showed that Lys289 (TM7) in the mouse P_{2U} receptor, corresponding to Gln296 (TM7) in the chick P_{2Y} receptor, when mutated to an arginine, reversed the selectivity of the triphosphates ATP and UTP to the corresponding diphosphates. In our proposed model Gln296 (TM7) is not in the vicinity of the phosphate BD, and this suggests that P_{2Y} and P_{2U} receptors display significantly different modes of binding of ligands, as implied by the pharmacology-derived nomenclature of the receptors.

Gln296 (TM7), in our model, is positioned in the vicinity of the N^6 amine of the adenine moiety. Substitution of the hydrogens on this amine with methyl groups, thus reducing the extent of the interaction between the N^6 region and Gln296 (the distance between the two increases), greatly decreases the activity of the analogues: N^6MeATP ($K_{0.5}$ ≈ 19 μM) is 6.8 times less potent than ATP ($K_{0.5}$ = 2.8 ± 0.7 μM.) and N^6diMeATP ($K_{0.5}$ ≈ 64 μM) is over 20-fold potent less than ATP in stimulating phospholipase C in turkey erythrocyte membranes.[10,14] The loss of affinity by the methyl substitution may, however, be compensated for by introducing an aromatic side chain on this substituent, as in N^6PEATP ($K_{0.5}$ = 7.1 ± 0.3 μM; only 2.5-fold less active than ATP). Such an aromatic substituent may be accommodated by residues Phe51 (TM1), Tyr100 (TM2), and Phe120 (TM3), which are located at distances ranging between 3.5 and 10 Å from the N^6 amine. Certain substituents on the 2-position of the adenine ring enhance activity, such as in 2MeSATP ($K_{0.5}$ = 8 ± 2 nM; 350-fold more potent than ATP) and APSATP ($K_{0.5}$ = 1.53 ± 0.21 nM; 1830-fold more potent than ATP).[14] Substituents in the 2-position may occupy the same region of the receptor as the N^6-substituents, as was proposed for the rat A_{2a} receptor,[54] or an entirely different region of the receptor as was proposed for the m3 muscarinic receptor.[55] In the latter case, the side chain would extend through a largely hydrophobia region accommodating the phenyl ring, into a more hydrophilic region occupied by the conserved aspartate in TM2 that confers allosteric regulation of α_2-adrenergic receptors by sodium,[53] where it could form a salt bridge with the amine. In our current model the phenyl ring of N^6PEATP occupies the same region as the phenyl ring of APSATP, thus adhering to the model proposed for the A_{2a} adenosine receptor.[54]

CONCLUSIONS

We have sought to identify positively charged amino acid residues (Arg or Lys) as anchoring points which could contribute major electrostatic interactions with the phosphates of ATP. Such residues should be conserved within the P_2 GPCR family and should also be pointing towards the center of the receptor cavity. Likewise, they should probably be located around the middle or upper third of the transmembrane regions, where most of the non-peptide GPCRs are thought to bind ligands. These requirements only yield two possible anchoring points: Lys269 in TM6 and Arg299 in TM7.

As a result of the above conclusions, we identified six more residues, Gln296 in TM7 in the adenine BD, Ser303 and Ser306 in TM7 in the ribose BD, His121 in TM3, His266 in TM6, and Tyr125 in TM3 in the triphosphate BD, that are involved in ligand binding according to this model. Furthermore, we have shown that our model is consistent with the current pharmacological data.

It will be interesting to construct models of the P_{2x} receptor, now cloned,[39–40] and compare the binding sites as a means of getting insights for achieving ligand selectivity.

Acknowledgments

The authors wish to thank Prof. H. Weinstein, Dr. J.A. Ballesteros and Ms. L. Laakonen of Mount Sinai Medical School, NY, and Dr. R. Pearlstein of the Division of Computer Research and Technology, NIH, MD, for their helpful suggestions towards this project. AMvR should like to thank Prof. G. Burnstock of University College London and the Cystic Fibrosis Foundation for financial support. The authors also wish to thank Dr. J.L. Boyer and Prof. T.K. Harden of the Univ. of North Carolina for the pharmacological determinations, which will be published in a separate study.

References

1. Burnstock, G. A basis for distinguishing two types of purinergic receptor. In: Straub, PW.; Bolis, L., editors. Cell Membrane Receptors for Drugs and Hormones: a Multidisciplinary Approach. New York: Raven Press; 1978. p. 106-118.
2. Hoyle, CHV. Transmission: purines. In: Burnstock, G.; Hoyle, CHV., editors. Autonomic neuroeffector mechanisms. Chun Harwood: Academic Press; 1992. p. 367-407.
3. Edwards FA, Gibb AJ, Colquhoun D. ATP receptor mediated synaptic currents in the central nervous system. Nature. 1992; 359:144–147. [PubMed: 1381811]
4. Hoyle, CHV.; Burnstock, G. ATP receptors and their physiological roles. In: Stone, TW., editor. Adenosine in the nervous system. London: Academic Press Ltd.; 1991. p. 43-76.
5. Cusack NJ. P_2, receptors: subclassification and structure-activity relationships. Drug Dev. Res. 1993; 28:244–252.
6. Gordon JL. Extracellular ATP: effects, sources and fate. J. Biochem. 1986; 223:309–319.
7. Fredholm BB, Abbracchio MP, Burnstock G, Daly JW, Harden TK, Jacobson KA, Leff P, Williams M. Nomenclature and classification of purinoceptors. Pharmacol. Rev. 1994; 46:143–156. [PubMed: 7938164]
8. Abbracchio MP, Burnstock G. Purinoceptors: are there families of P2X and P2Y purinoceptors? Pharmac. Ther. 1994; 64:445–475.
9. Dubyak GR. Signal transduction by P2-purinergic receptor for extracellular ATP. Am. J. Respir. cell. Mol. Biol. 1991; 4:295–300. [PubMed: 1707633]
10. Harden TK, Hawkins PT, Stephens L, Boyer JL, Downes P. Phosphoinositide hydrolysis by guanosine 5′([γ-thio]triphosphate)-activated phospholipase C of turkey erythrocyte membranes. Biochem. J. 1988; 252:583–593. [PubMed: 2843174]
11. Pirotton S, Bocynaems JM. Transduction mechanism of P_2 purinergic receptor: Role of phospholipase C and Calcium. Nucleos. Nucleot. 1991; 10:1009–1017.

12. Benham CD, Tsien RW. A novel receptor-operated Ca^{2+}-permeable channel activated by ATP in smooth muscle. Nature. 1987; 328:275–278. [PubMed: 2439921]
13. Bean BP. Pharmacology and electrophysiology of ATP activated ion channels. Trends Pharmacol. Sci. 1992; 13:87–90. [PubMed: 1374198]
14. Fischer B, Boyer JL, Hoyle CHV, Ziganshin AU, Brizzolara AL, Knight GE, Zimmet J, Burnstock G, Harden TK, Jacobson KA. Identification of potent, selective P_{2Y}-purinoceptor agonist structure-activity relationship for 2-thioether derivatives of adenosine 5′-triphosphate. J. Med. Chem. 1994; 36:3937–3946. [PubMed: 8254622]
15. Burnstock G, Fischer B, Hoyle CHV, Maillard M, Zinganshin AU, Brizzolara AL, Von Isakovics A, Boyer JL, Harden TK, Jacobson KA. Structure activity relationship for derivatives of adenosine 5′-triphosphate as agonists at P_2 purinoceptors; heterogeneity within P_{2X} and P_{2Y} subtypes. Durg Dev. Res. 1994; 31:206–219.
16. Windscheif U, Ralevic V, Bäurnert HG, Mutschler E, Lambrecht G, Burnstock G. Vasoconstrictor and vasodilator by responses to various agonists in the rat perfused mesenteric arterial bed – Selective-inhibition by PPADS of contractions mediated Via P_{2X}-purinoceptor. Br. J. Pharmacol. 1994; 113:1015–1021. [PubMed: 7858843]
17. Humphries RG, Tomlinson W, Ingall AH, Cage PA, Leff P. FPL-66096 – A Novel, highly potent and selective antagonist at human platelet P_{2T}-purinoceptors. Br J. Pharmacol. 1994; 113:1057–1063. [PubMed: 7858849]
18. Van Rhee AM, van der Heijden MPA, Beukers MPA, IJzerman AP, Soudijin W, Nickel P. Novel competitive antagonists for P_2 purinoceptor. Eur. J. Pharmacol. Mol. Pharmacol. Sect. 1994; 268:1–7.
19. Kyte J, Doolittle RF. A Simple method for displaying the hydrophobic character of protein. J. Mol. Biol. 1982; 157:105–132. [PubMed: 7108955]
20. Kubo T, Fukuda K, Mikama A, Maeda A, Takahashi H, Mishina M, Haga Y, Ichiyama A, Kangawa K, Kajima M, Matsuo H, Hirose T, Numa T. Cloning, sequencing and expressing of complementary DNA coding the muscarinic acetylcholine receptor. Nature. 1986; 323:411–416. [PubMed: 3762692]
21. Webb TE, Simon J, Krishek BJ, Bateson AN, Smart TG, King BF, Burnstock G, Barnard EA. Cloning and functional expression of a brain G-protein-coupled ATP receptor. FEBS Lett. 1993; 324:219–225. [PubMed: 8508924]
22. Filtz TM, Li Q, Boyer JL, Nicholas RA, Harden TK. Expression of a P_{2Y} purinergic receptor that couples to phospholipase C. Mol. Pharmacol. 1994; 40:8–14. [PubMed: 8058061]
23. Lustig KD, Shiau AK, Brake AJ, Julius D. Expression cloning of an ATP receptor from mouse neuroblastoma cells. Proc. Natl. Acad. Sci. USA. 1993; 91:5113–5117. [PubMed: 7685114]
24. Parr CE, Sullivan DM, Paradiso AM, Lazarowski ER, Burch LH, Olsen JC, Erb L, Weisman GA, Boucher RC, Tuner JT. Cloning and expression of a human P_{2U} nucleotide receptor, a target for cystic fibrosis pharmacotherapy. Proc. Natl. Acad. Sci. USA. 1994; 91:3275–3279. [PubMed: 8159738]
25. Rice WR, Burton FM, Fiedeldey DT. Cloning and expression of the alveolar type II cell P_{2U}-purinergic receptor. Am. J. Respir. Cell Mol. Biol. 1995; 12:27–32. [PubMed: 7811468]
26. Jacobson KA, Stiles GL, Ji XD. Chemical modification and irreversible inhibition of striatal A_{2a} adenosine receptors. Mol. Pharmacol. 1992; 42:123–133. [PubMed: 1635550]
27. Hibert MF, Trumpp-kallmeyer S, Bruinvels A, Hoflack J. Three-dimensional models of neurotransmitter G-binding protein-coupled receptors. Mol. Pharmacol. 1991; 40:8–15. [PubMed: 1649965]
28. Schertler GF, Villa C, Henderson R. Projection structure of rhodopsin. Nature. 1993; 362:770–772. [PubMed: 8469290]
29. Henderson R, Baldwin JM, Ceska TA, Zemlin F, Beckmann E, Downing KH. Model for the Structure of bacteriorhodopsin based on high-resolution electron crymicroscopy. J. Mol. Biol. 1990; 213:899–929. [PubMed: 2359127]
30. Oliveira L, Paiva ACM, Vriend G. A common motif in G-protein-coupled seven transmembrane helix receptors. J. Comp. Aided Mol. Design. 1993; 7:649–658.

31. Baldwin JM. The probable arrangement of the helices in G protein-coupled receptors. EMBO J. 1993; 12:1693–1703. [PubMed: 8385611]
32. Kovács T, Ötvös L. Simple synthesis of 5-vinly and 5-ethynyl-2'-deoxyuridine-5'-triphosphates. Tetrahedron Lett. 1988; 29:4525–4528.
33. Moffat JG. A general synthesis of nucleoside-5′-triphosphates. Can. J. Chem. 1964; 42:599.
34. Ballesteros JA, Weinstein H. Integrated methods for the construction of three dimensional models and computational probing of structure-function relations in G-protein coupled receptors. Method Neurosci. 1995; 25:366–428.
35. IJzerman AP, van Galen PJM, Jacobson KA. Molecular modeling of adenosine receptors. I. The ligand binding site on the A_1 receptor. Drug Des. Discov. 1992; 9:49–67. [PubMed: 1457698]
36. Zhang D, Weinstein H. Polarity conserved positions in transmembrane domains of G-protein coupled receptors and bacteriorhodopsin. FEBS Lett. 1994; 337:207–212. [PubMed: 8287978]
37. Sankararamakrishnan R, Vishveshwara S. Geometry of proline-containing alpha-helices in proteins. Int. J. Peptide Protein Res. 1992; 39:356–363. [PubMed: 1428525]
38. Noel JP, Hamm HE, Sigler PB. The 2.2 Å crystal structure of transducin-α complexed with GTPγS. Nature. 1993; 366:654. [PubMed: 8259210]
39. Brake AJ, Wagenbach MJ, Julius D. New structural motif for ligand-gated ion channels defined by an ionotropic ATP receptor. Nature. 1994; 371:519–523. [PubMed: 7523952]
40. Valera S, Hussy N, Evans RJ, Adami N, North RA, Surprenant A, Buell G. New class of ligand-gated ion-channel defined by P_{2X} receptor or extracellular ATP. Nature. 1994; 371:516–519. [PubMed: 7523951]
41. Erb L, Garrad R, Wang Y, Quinn T, Turner JT, Weisman GA. Site-directed mutagenesis of P_{2U} purinoceptors. J. Biol. Chem. 1995; 270:4185–4188. [PubMed: 7876172]
42. von Heijne G, Manoil C. Membrane proteins: from sequence to structure. Protein Eng. 1990; 4:109–112. [PubMed: 2075184]
43. Sander C, Schneider R. Database of homology-derived protein structures. Proteins. 1991; 9:56–68. [PubMed: 2017436]
44. Hoflack J, Trumpp-Kallmeyer S, Hibert M. Re-evaluation of bacteriorhodopsin as a model for G protein-coupled receptors. Trends Pharmacol. Sci. 1994; 43:348–350.
45. von Heijne G. Proline kinks in transmembrane α-helices. J. Mol. Biol. 1991; 218:499–503. [PubMed: 2016741]
46. Wess J, Gdula D, Brann MR. Site-directed mutagenesis of the m3 muscarinic receptor: identification of a series of threonine and tyrosine residues involved in agonist but not antagonist binding. EMBO J. 1991; 10:3729–3734. [PubMed: 1657592]
47. Suryanarayana S, Daunt DA, von Zastrow M, Kobilka BK. A point mutation in the seventh hydrophobic domain of the α_2 adrenergic receptor increases its affinity for a family of βreceptor antagonists. J. Biol. Chem. 1991; 266:15488–15492. [PubMed: 1678390]
48. Oksenberg D, Marsters SA, O'Dowd BF, Jin H, Havlik S, Peroutka SJ, Ashkenazi A. A single amino-acid difference confers major pharmacological variation between human and rodent 5-HT_{1B} receptors. Nature. 1992; 360:161–163. [PubMed: 1436092]
49. Fraser CM, Wang CD, Robinson DA, Gocayne JD, Venter JC. Site-directed mutagenesis of ml muscarinic acetylcholine receptors: conserved aspartic acids play important roles in receptor function. Mol. Pharmacol. 1989; 36:840–847. [PubMed: 2557534]
50. Elling CE, Møller Nielsen S, Schwartz TW. Conversion of antagonist binding site to metal-ion site in the tachykinin NK-1 receptor. Nature. 1995; 374:74–77. [PubMed: 7532789]
51. Kim J, Wess J, van Rhee AM, Schöneberg T, Jacobson KA. Site-directed mutagenesis identifies residues involved in ligand recognition in the human A_{2a} adenosine receptor. J. Biol. Chem. 1995; 270:13987–13997. [PubMed: 7775460]
52. Zhou W, Flanagan C, Ballesteros JA, Konvicka K, Davidson JS, Weinstein H, Millar RP, Sealfon SC. A reciprocal mutation supports helix 2 and helix 7 proximity in the gonadotropin-releasing hormone receptor. Mol. Pharmacol. 1994; 2:165–170. [PubMed: 8114667]

53. Horstman DA, Brandon S, Wilson AL, Guyer CA, Cragoe EJ, Limbird LE. An aspartate conserved among G-protein receptors confers allosteric regulation of α_2-adrenergic receptors by sodium. J. Biol. Chem. 1990; 265:21590–21595. [PubMed: 2174879]

54. IJzerman AP, van der Wenden EM, van Galen PJM, Jacobson KA. Molecular modeling of adenosine receptors – the ligand-binding site on the rat adenosine A_{2a} receptor. Eur. J. Pharmacol. Mol. Pharmacol Sect. 1994; 268:95–104.

55. Jacobson KA, Fischer B, van Rhee AM. Molecular probes for muscarinic receptors: functionalized congeners of selective muscarinic antagonists. Life Sci. 1995; 56:823–830. [PubMed: 10188781]

56. Boyer JL, Harden TK, Fischer B, Jacobson KA. in preparation.

List of Abbreviations

all single and three letter notations for amino acids.

2MeSATP	2-methylthioadenosine 5'-triphosphate
APSATP	2-(2-(4-aminophenyl)ethyl)thio-adenosine 5′-triphosphate
ATP	adenosine 5′-triphosphate
BD	binding domain
cAMP	adenosine 3′,5′-cycle monophosphate
CG	Conjugate Gradient
GPCR	G-protein coupled receptor
MNDO	Medium Neglect of Differential Overlap
N^6diMeATP/ N^6diMeAMP	N^6,N^6-dimethyl-adenosine 5′-triphosphate/-monophosphate
N^6PEATP/N^6PEAMP	N^6-(2-phenylethyl)-adenosine 5′-triphosphate/-monophosphate
PDB	Protein Database Brookhaven
r.m.s	root mean square
TBAP	tetrabutylammonium phosphate
TEAB	triethylammonium bicarbonate
TM	transmembrane domain
UTP	uridine 5′-triphosphate

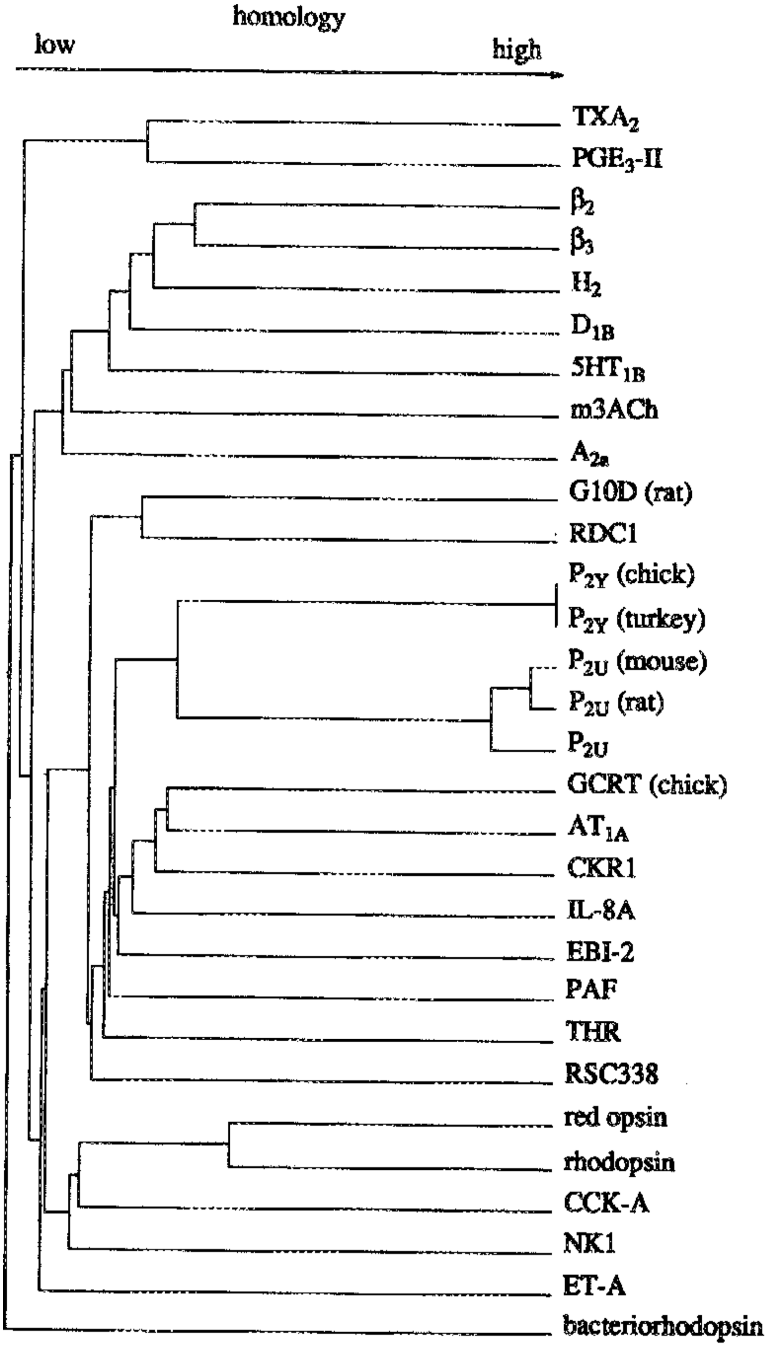

index	subtype	species	accession no.
TXA2	TXA_2	human	P21731
PGE3-II	PGE_3-II	human	L27488
B2AR	β_2AR	human	P07550
B3AR	β_3AR	human	P13945
H2	H_2	human	P25021
D1B	D_{1B}	human	P21918
5HT1B	$5HT_{1B}$	human	P28222
m3ACh	m3ACh	human	P20309
A2a	A_{2a}	human	P29274
G10D	G10D	rat	P31392
RDC1	RDC1	human	P25106
GCRT	GCRT	chicken	P32250
AT1A	AT_{1A}	human	P30556
CKR1	CKR1	human	P32246
IL-8A	IL-8A	human	P25024
EBI2	EBI2	human	P32249
cP2Y	P_{2Y}	chicken	P34996
tP2Y	P_{2Y}	turkey	U09842
P2U	P_{2U}	human	L14751
MP2U	P_{2U}	mouse	P35383
rP2U	P_{2U}	rat	U09402
PAF	PAF	human	P25105
THR	thrombin	human	P25116
RSC338	RSC338	human	D13626
ops	red opsin	human	P04000
rho	rhodopsin	human	P08100
CCK-A	CCK-A	human	P32238
NK2	NK2	human	P21452
ET-A	ET-A	human	P25101

Figure 1.

Dendrogram for selected G-protein coupled receptors, including the Known P_2 receptor sequences.

Dendrogram and included sequences.

TM1			
cP2Y	40	FYYLPTVYILVFITGFLGNSVAIWMFVFHMR	70
tP2Y	40	FYYLPTVYILVFITGFLGNSVAIWMFVFHMR	70
P2U	33	YVLLPVSYGVVCVLGLCLNAVGLYIFLCRLK	63
mP2U	33	YVLLPVSYGVVCVLGLCLNVVALYIFLCRLK	63
rP2U	33	YVLLPVSYGVVCVLGLCLNVVALYIFLCRLK	63
A2a	6	SSVYITVELAIAVLAILGNVLVCWAVWLNSN	36
NK1	32	IVLWAAAYTVIVVTSVVGNVVVIWIILAHKR	62
AT1A	28	FVMIPTLYSIIFVVGIFGNSLVVIVIYFYMK	58
PAF	15	YTLFPIVYSIIFVLGVIANGYVLWVFARLYP	45
THR	102	TLFVPSVYTGVFVVSLPLNIMAIVVFILKMK	132
m3ACh	68	VVFIAFLTGILALVTIIGNILVIVSFKVNKQ	98
rho	37	FSMLAAYMFLLIVLGFPINFLTLYVTVQHKK	67
bacr	22	EWIWLALGTALMGLGTLYFLVKGMGVSDPDA	52
TM2			
cP2Y	76	SVYMFNLALADFLYVLTLPALIFYYFNK	103
tP2Y	76	SVYMFNLALADFLYVLTLPALIFYYFNK	103
P2U	69	TTYMFHLAVSDALYAASLPLLVYYYARG	135
mP2U	69	TTYMFHLAVSDSLYAASLPLLVYYYARG	96
rP2U	69	TTYMFHLAVSDSLYAASLPLLVYYYAQG	96
A2a	42	NYFVVSLAAADIAVGVLAIPFAITISTG	69
NK1	68	NYFLVDLAFAEACMAAFNTVVNFTYAVH	95
AT1A	64	SVFLLNLALADLCFLLTLPLWAVYTAME	91
PAF	53	KIFMVNLTMADMLFLITLPLWIVYYQNQ	80
THR	138	VVYMLHLATADVLFVSVLPFKISYYFSG	165
m3ACh	104	NYFLLSLACADLIIGVISMNLFTTYIIM	131
rho	73	NYILLNLAVADLFMVLGGFTSTLYTSLH	100
bacr	49	DPDAKKFYAITTLVPAIAFTMYLSMLLG	76
TM3			
cP2Y	114	KLQRFIFHVNLYGSILFLTCISVHR	138
tP2Y	114	KLQRFIFHVNLYGSILFLTCISVHR	138
P2U	107	KLVRFLFYTNLYCSILFLTCISVHR	131
mP2U	107	KLVRFLFYTNLYCSILFLTCISVHR	131
rP2U	107	KLVRFLFYTNLYCSILFLTCISVHR	131
A2a	78	LFIACFVLVLTQSSIFSLLAIAIDR	102
NK1	106	KFHNFFPIAAVFASIYSMTAVAFDR	130
AT1A	102	KIASASVSFNLYASVFLLTCLSIDR	126
PAF	91	NVAGCLFFINTYCSVAFLGVITYNR	115
THR	176	RFVTAAFYCNMYASILLMTVISIDR	200
m3ACh	142	DLWLAIDYVASNASVMNLLVISFDR	166
rho	111	NLEGFFATLGGEIALWSLVVLAIER	135
bacr	89	NPIYWARYADWLFTTPLLLLDLALL	113
TM4			
cP2Y	153	KKKNAVYVSSLVWALVVAVIAPILFYS	179
tP2Y	153	KKKNAVYVSSLVWALVVAVIAPILFYS	179
P2U	146	RARYARRVAGAVWVLVLACQAPVLYFV	172
mP2U	146	RARYARRVAAVVWVLVLACQAPVLYFV	172
rP2U	146	HARYARRVAAVVWVLVLACQTPVLYFV	172
A2a	117	TGTRAKGIIAICWVLSFAIGLTPMLGW	143
NK1	143	SATATKVVICVIWVLALLLAFPQGYYS	169
AT1A	141	TMLVAKVTCIIIWLLAGLASLPAIIHR	167
PAF	129	NTRKRGILSLVIWVAIVGAASYFLILD	155
THR	215	TLGRASFTCLAIWALAIAGVVPLVLKE	241
m3ACh	181	TTKRAGVMIGLAWVISFVLWAPAILFW	207
rho	149	GENHAIMGVAFTWVMALACAAPPLAGW	175
bacr	116	ADNGTILALVGADGIMIGTGLVGALTK	142

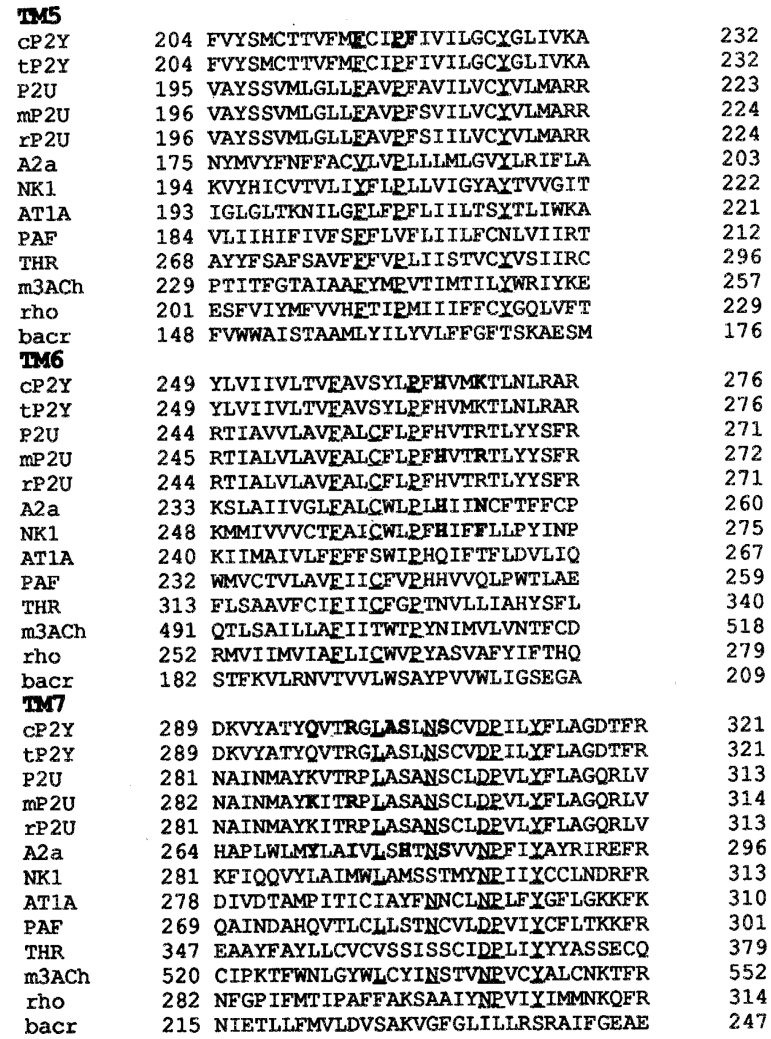

Figure 2.

Alignment of putative transmembrane domains, constructed as described in Materials and Methods and allowing no gaps in the sequence. Human sequences, where available, were used. In addition to the receptors shown: TXA_2, PGE_3-II, β_2AR, β_3AR, H_2, D_{1B}, $5HT_{1B}$, G10D, RDC1, GCRT, CKR1, IL-8A, EBI2, RSC338, red opsin, CCK-A, NK2, ET-A, and bacteriorhodopsin were also used in the alignment (see Figure 1). Unless specified, sequences are from the human, c = chick, t = turkey, m = mouse, r = rat. The residues of the alignment motifs are underlined, and the discussed in this paper are printed in bold type.

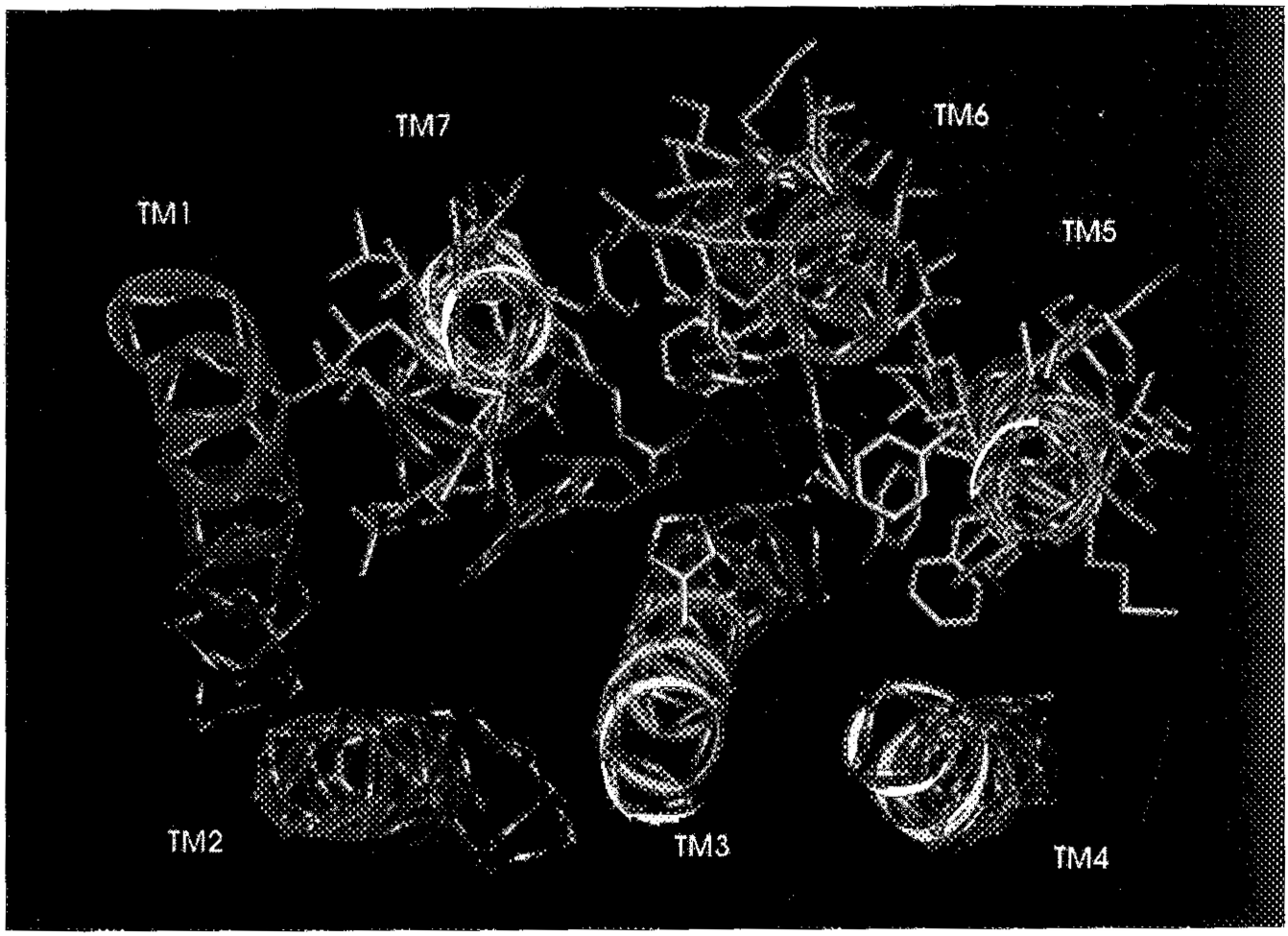

Figure 3.
View of the helical bundle of the chick $P2Y_1$ receptor from the luminal side. Displayed (and coloured by atom type) are the helix backbone atoms, the side chains of TMs 5–7, and His121 in TM3. The adenosine moiety of ATP is displayed in dark green, and the triphosphate chain in purple. (See Color Plate IV at back of this issue).

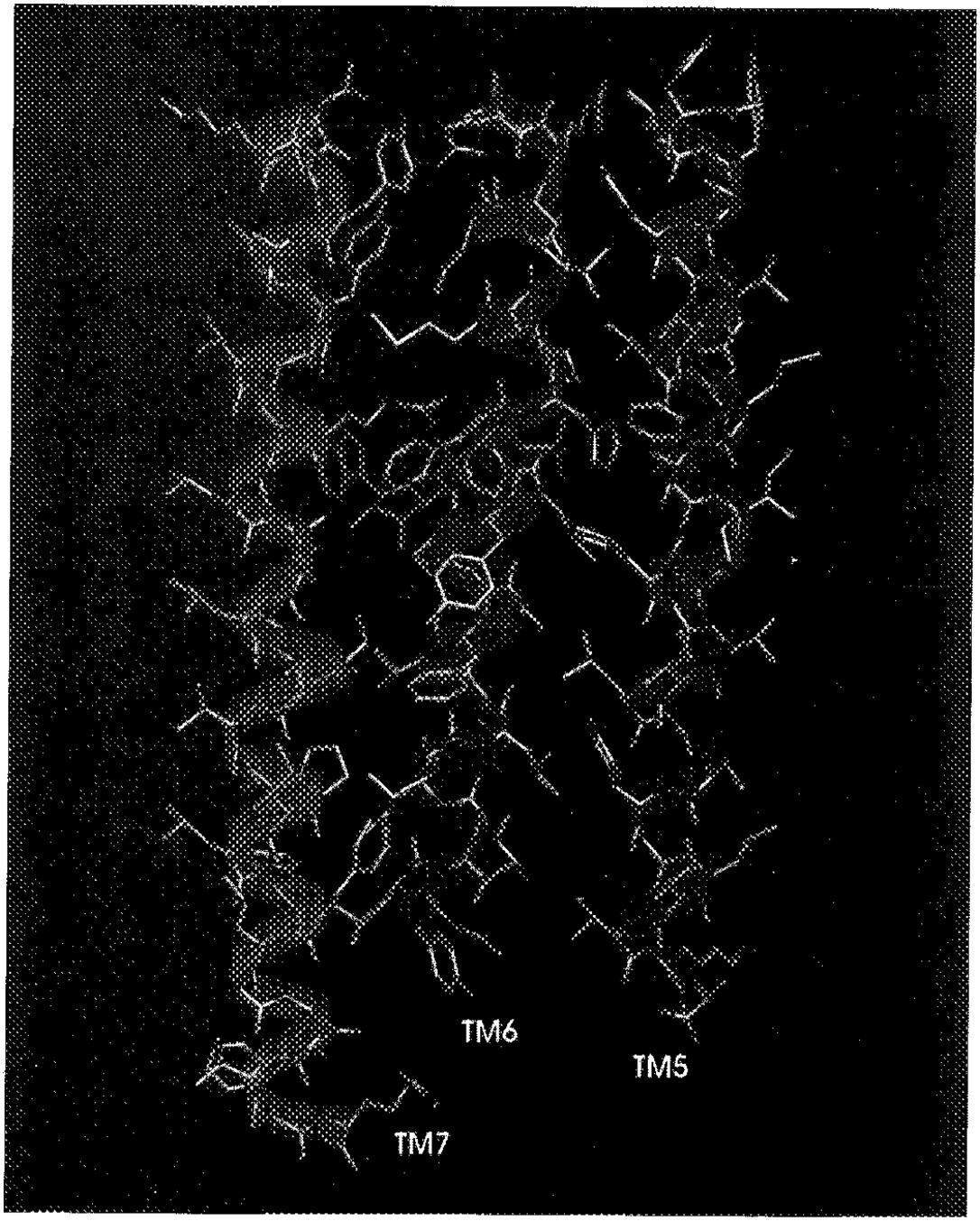

Figure 4.
TMs 5–7 and ATP, as viewed in the plane of the membrane along the short axis. The adenosine moiety of ATP is displayed in dark green, and the triphosphate chain in purple. (See Color Plate V at back of this issue).

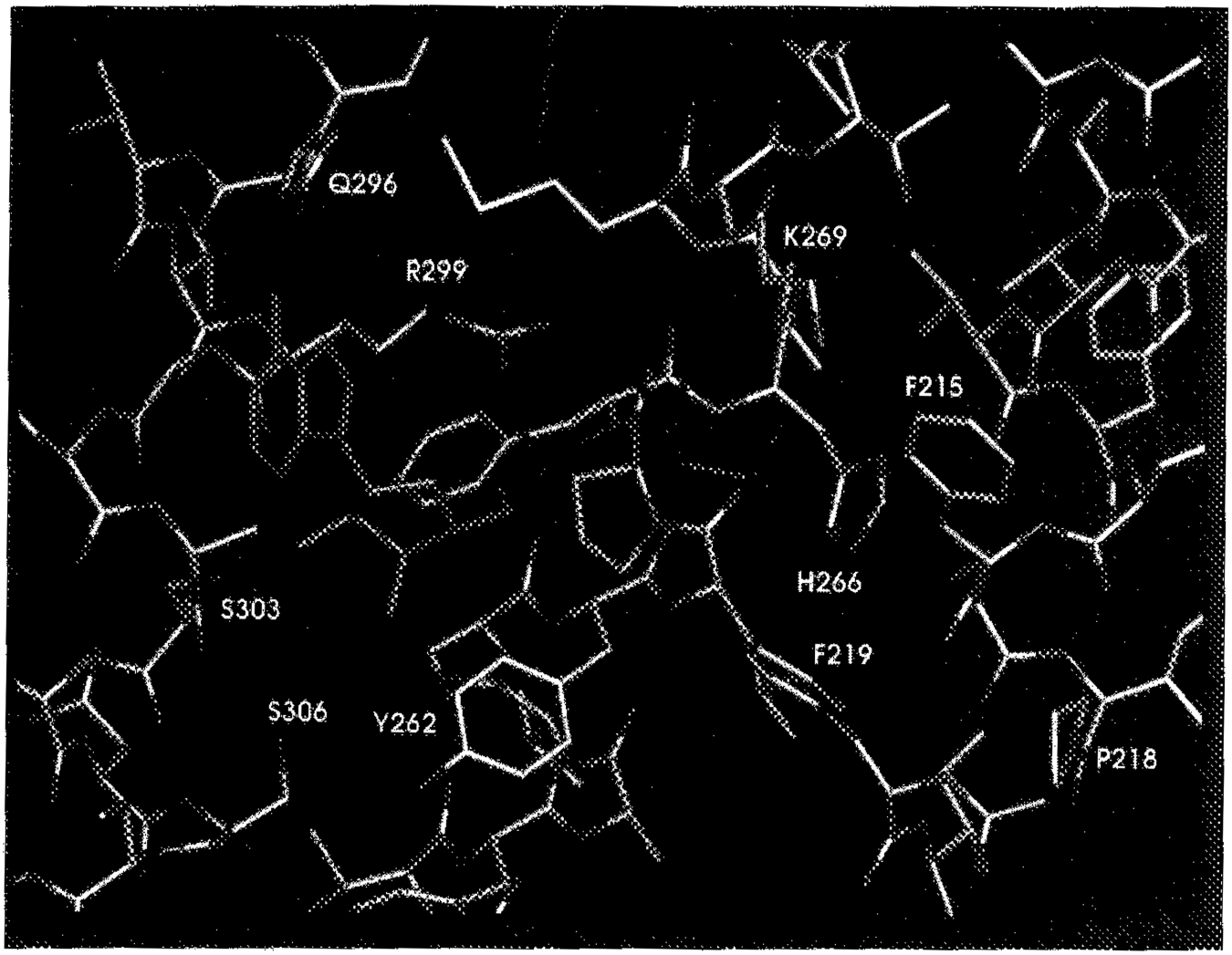

Figure 5.
Display of TMs 5–7 and ATP, in the vicinity of the binding site. The adenosine moiety of ATP is displayed in dark green, and the triphosphate chain in purple. (See Color Plate VI at back of this issue).